 ISSN 0267-8179. DOI: 10.1002/jqs.1533

Holocene changes in precipitation seasonality in the western Mediterranean Basin: a multi-species approach using $\delta^{13}C$ of archaeobotanical remains

M. AGUILERA,[1] J. P. FERRIO,[2] G. PÉREZ,[3] J. L. ARAUS[1] and J. VOLTAS[2]*
[1]Unitat de Fisiologia Vegetal, Facultat de Biologia, Universitat de Barcelona, Avda. Diagonal 645, 08028 Barcelona, Spain
[2]Department of Crop and Forest Sciences, University of Lleida, Spain
[3]Grupo de Investigación Arqueobotánica, Instituto de Historia, CCHS-CSIC, Madrid

Received 30 March 2011; Revised 21 June 2011; Accepted 25 June 2011

ABSTRACT: Precipitation has been of utmost importance in shaping the evolution of landscapes and human settlements in the Mediterranean. However, information on seasonal precipitation patterns through the Holocene is scarce. This study attempts to quantify the evolution of seasonal precipitation in the East Iberian Peninsula (5000 BC to AD 600) based on the carbon isotope composition ($\delta^{13}C$) of archaeobotanical remains. Data on Holm oak, Aleppo pine and small-grain cereals were combined, and precipitation was inferred from models relating present-day records to the $\delta^{13}C$ of modern samples. Subsequently, charred grains were used as a proxy for ancient moisture during April–May, whereas oak and pine charcoals provided complementary rainfall estimates for September–December and January–August, respectively. The results reveal aridity changes throughout the Holocene in the western Mediterranean. Past spring–summer precipitation was consistently higher than at present. In contrast, autumn and early winter precipitation showed stronger fluctuations, particularly during the first millennium BC, and often exhibited values below those of the present. The high contribution of autumn precipitation to the annual water budget, typical of the present Mediterranean climate, was definitively established at the beginning of the current era. This study shows how a combination of species holding complementary environmental signals can contribute to a wider knowledge of local precipitation dynamics. Copyright © 2011 John Wiley & Sons, Ltd.

KEYWORDS: carbon isotopes; charred grains; *Pinus halepensis*; *Quercus ilex*; Iberian Peninsula.

Introduction

The western Mediterranean is characterized by the interaction of African subtropical, North Atlantic and Mediterranean climate systems (Rodó *et al.*, 1997; Dunkeloh and Jacobeit, 2003). These influences control climate variability in the region, producing singular environmental conditions throughout the Holocene (Araus *et al.*, 1997; Jalut *et al.*, 1997; Magny *et al.*, 2002, 2003). Precipitation has been of utmost importance in shaping the evolution of landscapes and human settlements in the area (Jalut *et al.*, 1997; Sanchez-Goni *et al.*, 2002; Barriendos and Llasat, 2003; Valero-Garcés *et al.*, 2004). Several multidisciplinary studies have addressed the pace of climate changes in the Mediterranean Basin for the last millennia, although mid- and late-Holocene proxy records for Spain are scarce. Lake sediment (Vegas *et al.*, 2001; Moreno *et al.*, 2005), as well as palynological (Pérez-Obiol and Julià, 1994; Jalut *et al.*, 2000) and hydrological studies (Roberts *et al.*, 2008) have been successfully used to gain insight into past climate, but they provide qualitative information that may warrant further validation. In recent years, stable isotopes have become widely used in palaeoenvironmental research (McCarroll and Loader, 2004); in particular, carbon isotope composition ($\delta^{13}C$) is being routinely used for dry environments (Araus *et al.*, 1997; Voltas *et al.*, 2008) as $\delta^{13}C$ values are very sensitive to drought. Previous work suggests that $\delta^{13}C$ records of archaeobotanical remains (either charcoal wood or charred cereal grains) provide valuable environmental information, even of a quantitative nature, that is useful for reconstructing Holocene aridity changes (e.g. Ferrio *et al.*, 2005, 2006).

The imprint of water availability on plant $\delta^{13}C$ in arid and semi-arid regions has been reported elsewhere (e.g. Williams and Ehleringer, 2000; Warren *et al.*, 2001). Under water stress, stomatal closure reduces intercellular CO_2 concentration and limits CO_2 availability for the carboxylating enzyme (Rubisco), which is forced to fix a greater proportion of the heavier carbon isotope (^{13}C), thus increasing $\delta^{13}C$ (Farquhar *et al.*, 1982). In this regard, wood $\delta^{13}C$ has been related to climatic variables that influence plant water status (Dupouey *et al.*, 1993; Korol *et al.*, 1999; Ferrio *et al.*, 2003; Klein *et al.*, 2005), whereas kernel $\delta^{13}C$ of small-grain cereals is closely associated with water availability from anthesis to maturity (Araus *et al.*, 1997, 2003; Voltas *et al.*, 1999). Interestingly, co-occurring tree species may show a differential response to seasonal patterns of water availability (Flanagan *et al.*, 1992; Valentini *et al.*, 1994; Ferrio *et al.*, 2003), and thus their $\delta^{13}C$ values can provide complementary climatic information (Ferrio *et al.*, 2007).

For extracting reliable palaeoclimatic information from $\delta^{13}C$ of archaeobotanical material it is compulsory to check and, eventually, correct for significant shifts in the original $\delta^{13}C$ after charring. Contradictory results have been obtained so far on the effect of carbonization on wood, probably owing to both its chemical complexity and the associated biogeochemical process occurring during charring. Depending on charring conditions and species, results have shown enrichment, depletion or no change in $\delta^{13}C$ (Jones and Chaloner, 1991; Czimczik *et al.*, 2002; Turney *et al.*, 2006; Ferrio *et al.*, 2007; Resco *et al.*, 2011). Fortunately, charcoal $\delta^{13}C$ is still strongly related to the original wood $\delta^{13}C$ in conifers such as *Pinus halepensis*, and changes due to carbonization can be corrected by taking the charcoal %C as an indicator of the degree of carbonization (Ferrio *et al.*, 2006). This remains to be more widely tested in hardwoods, which have different chemical and physical wood properties and have shown contrasting responses (Czimczik *et al.*, 2002; Turney *et al.*, 2006; Ferrio *et al.*, 2007). Conversely, several studies have demonstrated that the original isotopic signal remained unaffected in cereal grains following experimental charring (e.g. Marino and DeNiro, 1987; Araus and Buxó, 1993).

The investigations described here were aimed at obtaining evidence supporting the existence of changes in aridity throughout the mid- and late-Holocene in the western

*Correspondence: J. Voltas, as above.
E-mail: jvoltas@pvcf.udl.es

Mediterranean Basin (Valencia Province, eastern Spain). In particular, we attempted to reconstruct quantitatively the evolution of seasonal (autumn, spring, winter–summer) and annual precipitation during the period 5000 BC to AD 600 (from Neolithic to Visigoth periods) based on $\delta^{13}C$ evidence. To this end, data on Holm oak, Aleppo pine and small-grain cereals were combined. Fossil grains were used as a proxy for ancient moisture conditions during mid-spring (second half of April plus May) (Araus *et al.*, 1997; Ferrio *et al.*, 2005), whereas Holm oak and Aleppo pine charcoals provided complementary records of changes in seasonal (September–December and January-August for pines and oaks, respectively) and annual precipitation. Together, both types of records allow valuable information on changes in rainfall seasonality dynamics through time to be retrieved.

Materials and methods

Archaeobotanical material

Charred grains of hulled barley (*Hordeum vulgare* L.) and naked wheat (*Triticum aestivum/durum*, after Van Zeist and Bakker-Heeres), and charcoal fragments of Holm oak/Kermes oak (*Quercus ilex/coccifera*) and Aleppo pine (*Pinus halepensis* Mill.) were recovered from 17 archaeological sites in two nearby zones located north and south of Valencia Province (eastern Iberian Peninsula) (Fig. 1). One is in the Túria valley (north of Valencia Province; five sites); the other zone corresponds to the head of several valleys (Serpis, Canyoles and Albaida) in the Pre-Betic mountain range (south of Valencia – north of Alicante; 11 sites), with the exception of Alt de Benimaquia, located near the Mediterranean coast. These zones are separated physically by the Caroig Massif, a calcareous mountain range with its highest point at 1120 m a.s.l. The maximum distance between zones is about 70 km. Within each zone, the maximum distance between archaeological sites is 40 and 70 km for the Túria valley and the Pre-Betic range, respectively. The sites were selected based on the availability of archaeobotanical remains for these species, which cover a temporal range of nearly six millennia, from the Early Neolithic (5058 cal a BC) to the Visigoth period (AD 600). Sites of the Pre-Betic range provided remains covering almost five millennia, from 5058 cal a BC (Early Neolithic; Cova de l'Or, one of the earliest agricultural settlements of the Iberian Peninsula) to AD 200 (Roman period), whereas sites in the Túria valley supplied more recent material, from 1764 cal a BC (Bronze Age) to AD 600 (Visigoth).

At present, the sites are characterized by a semi-arid Mediterranean climate, with annual rainfall ranging from 429 to 751 mm (Table 1) and mean annual temperature from 14 to 18°C. Current meteorological data (mean monthly maximum and minimum temperature and monthly precipitation) of each archaeological site were obtained for the period 1950–1999 from the Digital Climatic Atlas of the Iberian Peninsula (Ninyerola *et al.*, 2005) implemented in MiraMon-GIS with a spatial resolution of 200 m. Present-day natural vegetation is typical Mediterranean, with Aleppo pine, Holm oak and shrubs and herbaceous plants such as Kermes oak, strawberry tree, juniper, rosemary, common thyme and rockrose.

Charred grains and charcoal remains were found as residues of domestic fires or preserved as carbonized elements after a settlement's destruction by fire. *Q. ilex* and *Q. coccifera* are evergreen Mediterranean oaks, but they are impossible to differentiate based on the anatomical features of charcoal. This may introduce uncertainties related to the proper characterization of modern material for palaeoclimatic inference, but *Q. ilex* (a medium-sized tree that is today more abundant in eastern Spain than the shrubby *Q. coccifera*) has a potentially much wider variety of end-uses by ancient communities (Cortijo, 2007; Buxó and Piqué, 2008). Presumably, these early communities gathered *P. halepensis* and *Q. ilex/coccifera* close to their settlements, given the dominance of these species in arboreal pollen records for the area (Carrión and Van Geel, 1999; Fernández *et al.*, 2007). To recover plant remains, soil samples were treated using a standard flotation tank with 5-, 2- and 0.5-mm sieves. The exception was for Cova de l'Or, at which a dry sieving procedure was followed. The average size of charcoal fragments for isotope analysis was $6 \times 4 \times 3$ mm and the estimated mean number of tree rings per fragment was 7.6 ± 6.5 (SD). Each charcoal or charred grain was soaked separately with 6 M HCl for 24 h at room temperature to remove carbonate crusts (DeNiro and Hastorf, 1985), which is a crucial step to avoid $\delta^{13}C$ shifts, and then rinsed repeatedly with distilled water. Finally, charcoals and charred grains were oven dried and milled separately for isotope analysis.

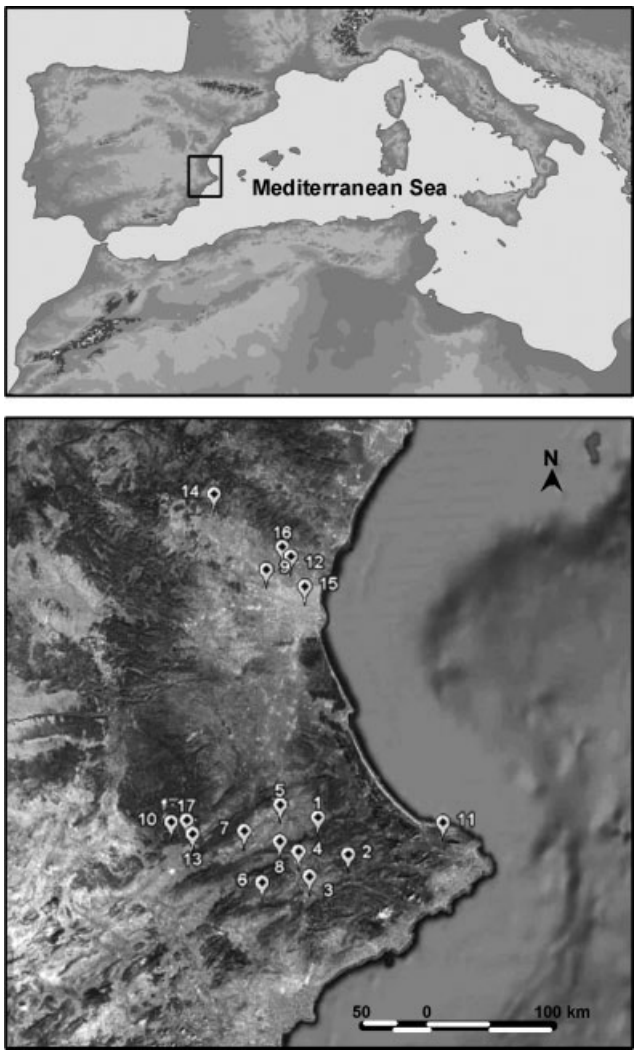

Figure 1. Location of the 17 archaeological sites on the Iberian Peninsula.

For the sites from the Early Neolithic and Late Bronze Age periods, radiocarbon ages were determined at Beta Analytical Inc. (Miami, FL, USA) or at the Oxford Radiocarbon Accelerator Unit (Oxford, UK), and calibrated dates were obtained by using the CalPal-2007 software (Weninger *et al.*, 2007). Because radiocarbon dating of each plant fragment was not realistic, we assigned instead an average date to each stratigraphic unit. For dating the more recent sites, a combination of stratigraphic and

Table 1. Site of origin and coding, annual precipitation and chronological dating of archaeobotanical remains.

Code	Site	Precipitation (mm)	Calendar year (BC/AD)
1	Cova de l'Or	604	5058 ± 167 cal a BC
2	Cova de Sta Maira	751	4472 ± 68 cal a BC
3	Mas d'Is	522	4400 ± 50 cal a BC
4	Les Jovades	594	3516 ± 74 cal a BC
5	Colata (MTV)	611	3249 ± 300 cal a BC
			3107 ± 190 cal a BC
6	Abric de la Falguera	507	2871 ± 164 cal a BC
			1750 ± 500 BC
7	Arenal de la Costa	555	2097 ± 57 cal a BC
8	Mola d'Agres	718	2225 ± 63 cal a BC
			1850 ± 350 BC
9	Lloma de Betxí	442	1764 ± 96 cal a BC
			1490 ± 70 cal a BC
10	Arbocer	508	1400 ± 100 BC
11	Alt de Benimaquia	727	623 ± 99 cal a BC
12	Tos Pelat	440	375 BC
13	Bastida	460	325 BC
14	Castellet de Bernabé	429	200 BC
15	Almoina	460	120 BC
			AD 40
16	Horta Vella	488	AD 100
			AD 450
			AD 485
			AD 600
17	Faldetes	554	AD 200

See supporting Table S1 for additional details.

archaeological methods was used (Table 1 and Supporting information, Table S1).

Reference material

To assess the effect of precipitation on $\delta^{13}C$ of modern wood material, we selected sampling sites representative of the distribution area of *P. halepensis* and *Q. ilex* in Spain. The number of sampling sites was 23 and 31 for *P. halepensis* and *Q. ilex*, respectively, and wood cores were obtained for at least five dominant trees per site. For $\delta^{13}C$ analysis, a fragment of the cores corresponding to the periods 1975–1999 and 1980–2001 was selected for *P. halepensis* and *Q. ilex*, respectively. Extended details on the sampling procedure and sample preparation can be found in Ferrio *et al.* (2003) and Aguilera *et al.* (2009). In turn, the precipitation signal recorded in wheat and barley grains was characterized using reference material taken from rain-fed field trials (12 for wheat, *T. aestivum* and *T. durum*; 20 for barley) as described elsewhere (Araus *et al.*, 1997, 2003; Voltas *et al.*, 1999; Ferrio *et al.*, 2001).

Interspecific comparisons of $\delta^{13}C$ records were performed whenever modern samples of different species (including both forest trees and cereals) co-occurred in particular geographical origins. As *P. halepensis* and *Q. ilex* did not co-occur in any of the aforementioned sampling sites, 18 additional sites showing the coexistence of both species were sampled. They represent most of the variation range in thermal and precipitation regimes along which *P. halepensis* and *Q. ilex* coexist in Spain. The cores, originating from five healthy and dominant trees, were obtained with a Trephor tool (Rossi *et al.*, 2006). They were 2 mm in diameter and about 15 mm in length, and contained the most recently formed tree rings. Visual tree-dating of the most recent tree rings was performed with a binocular microscope. The number of tree rings included in *P. halepensis* and *Q. ilex* segments averaged 9 ± 3 and 27 ± 8 (SD), respectively. In the case of cereals, a subset of seven rain-fed locations where both wheat and barley were tested in adjacent field trials was selected for comparison of $\delta^{13}C$ patterns. In some instances, crop and forest trees were subjected to pair-wise $\delta^{13}C$ comparison. This was done when the geographical distance between a field trial (for cereals) and a sampling site (for trees) was less than 10 km, which was considered as a threshold guaranteeing nearly uniform climatic conditions. Each modern sample was oven-dried at 65°C for 48 h and milled separately to a fine powder prior to isotopic analysis.

Charring effects on wood $\delta^{13}C$

The original wood $\delta^{13}C$ ($\delta^{13}C_w$) for *P. halepensis* was estimated following the model developed by Ferrio *et al.* (2006) for correction of the effect of carbonization on the isotopic signature, which uses charcoal $\delta^{13}C$ ($\delta^{13}C_{ch}$) and charcoal carbon concentration ($\%C_{ch}$):

$$\delta^{13}C_w = 0.706 \times \delta^{13}C_{ch} + 0.031 \times \%C_{ch} - 8.07. \quad (1)$$

The impact of carbonization on wood $\delta^{13}C$ of hardwoods seems less clear. Previous results of experimental charring of several species (including deciduous and evergreen oaks) collected along geographical gradients have shown non-significant shifts in $\delta^{13}C$ (Ferrio *et al.*, 2007), but other studies have reported consistent $\delta^{13}C$ changes in response to different carbonization treatments (Turney *et al.*, 2006). Here we performed a thorough assessment of the impact of carbonization on Holm oak $\delta^{13}C$. To this end, wood samples were collected from 12 sites in eastern Spain: two cores of 5 mm diameter were extracted from the south side of three mature, healthy and dominant trees per site. Visual tree-ring dating was performed with a binocular microscope, and the last 20 rings were identified and excised from each core. One segment per tree was then reduced to fine powder using a ball mill (Retsch MM301, Haan, Germany) and divided into two subsamples; the other segment was kept intact. While one powdered subsample was used as control for isotopic analysis, the other subsample and its matching intact segment were wrapped individually in aluminium foil and placed on porcelain crucibles. This was done to reproduce the anoxic conditions in which wood becomes charcoal instead of being combusted, either in the form of wood powder (Turney *et al.*, 2006) or as intact fragments, to emulate the conditions of a forest or cooking fire (Ferrio *et al.*, 2006). Wrapped samples were then subjected to one of three distinct temperatures (300, 400 or 500°C; one temperature for each tree from every sampling site) in an already heated muffle furnace for 30 min. The temperatures were chosen to provide material that varied in the degree of carbonization, ranging from slightly charred to fully carbonized (at the limit of total combustion). After this period, the charred intact segments were also milled to fine powder.

Stable isotope analysis

For the determination of $\delta^{13}C$, an aliquot of each sample (including modern, archaeological and experimentally charred material) was weighed into tin foil capsules and combusted using an elemental analyser interfaced to an isotope ratio mass spectrometer at Iso-Analytical (Sandbach, UK). Isotope ratios were expressed as per mille deviations using the δ notation relative to the VPDB standard. The accuracy of analyses was 0.06‰. Carbon isotope discrimination ($\Delta^{13}C$) was calculated from $\delta^{13}C$ values and $\delta^{13}C$ of atmospheric CO_2 ($\delta^{13}C_{air}$), as

described by Farquhar *et al.* (1982):

$$\Delta^{13}C = \frac{\delta^{13}C_{air} - \delta^{13}C}{1 + \delta^{13}C}. \quad (2)$$

To account for changes in air $\delta^{13}C$ during the Holocene, $\delta^{13}C_{air}$ for archaeological samples was inferred by interpolating data from Antarctic ice-core records, together with modern data from two Antarctic stations (Halley Bay and Palmer Station) of the CU-INSTAAR/NOAA-CMDL network. At present, Antarctic records provide the most extensive evidence of long-term global $\delta^{13}C_{air}$ changes. A smoothed $\delta^{13}C$ curve of atmospheric CO_2 from 16 100 BC to the present is available at http://web.udl.es/usuaris/x3845331/AIRCO2_LOESS.xls. According to this model the estimated $\delta^{13}C_{air}$ for archaeobotanical material ranged from −6.52 to −6.30‰.

Estimation of water inputs from $\Delta^{13}C$ of grain cereals

$\Delta^{13}C$ of cereal grains presents a strong positive relationship with water inputs (WI) (precipitation or precipitation plus irrigation) during grain filling. Past water inputs (mm) were estimated as follows (Araus *et al.*, 1997, 1999; Ferrio *et al.*, 2005):

$$WI_{wheat} = 0.225 \times e^{(0.364 \times \Delta 13C)} \quad (n = 25,\ r^2 = 0.73,\ P < 0.001) \quad (3)$$

$$WI_{barley} = 0.175 \times e^{(0.376 \times \Delta 13C)} \quad (n = 22,\ r^2 = 0.73,\ P < 0.001). \quad (4)$$

Total precipitation during grain filling was obtained for the second half of April plus May period (Araus *et al.*, 1997).

Estimation of annual and seasonal precipitation from charcoal $\Delta^{13}C$

Linear regression models were developed relating annual and seasonal precipitation to wood $\Delta^{13}C$ of modern material (either Q. *ilex* or *P. halepensis*) as described previously (Ferrio *et al.*, 2003; Ferrio and Voltas, 2005; Aguilera *et al.*, 2009). Briefly, we first selected the best fitting monthly precipitation model from $\Delta^{13}C$ of *Q. ilex* (October) as starting point, with a number of combinations of consecutive months also tested for further inferences based on $\Delta^{13}C$. For selection purposes, a leave-one-out cross-validation was applied, and September–December was chosen as the period providing best precipitation estimates for *Q. ilex*. Based upon this realization, the complementary year period (comprising January–August) was proposed as candidate model for seasonal precipitation inferences in the case of *P. halepensis* (decision stemming from earlier evidence on the sensitivity of *P. halepensis* to monthly precipitation; Ferrio *et al.*, 2003; Ferrio and Voltas, 2005). Finally, the hypothetically complementary seasonal precipitation signal stored in *Q. ilex* and *P. halepensis* was confirmed by examining coefficients of determination (R^2) of linear regressions for each year period.

The present coexistence of *P. halepensis* and *Q. ilex* occurs under varying patterns of precipitation seasonality accompanied by a regular incidence of summer drought. These climate conditions define the ecological niches of these widely distributed Mediterranean trees, which show a long-term presence and adaptation to the Mediterranean Basin (e.g. Lumaret *et al.*, 2002; Grivet *et al.*, 2011). For inferences on past conditions, we presumed that present associations between seasonal precipitation and $\Delta^{13}C$ of woody species would essentially hold in the past given the very wide climatic range of calibration sites, potentially covering most scenarios of past seasonal precipitation variability.

Statistical analyses

The experimental charring data were subjected to three-way ANOVA to determine the effect of carbonization at three different temperatures (300, 400 and 500°C) and in different sample types (milled or intact wood), as well as to ascertain the relevance of the geographical origin, on the $\delta^{13}C$ and %C of wood. For all pair-wise species combinations, the $\Delta^{13}C$ values of charred remains originating from common stratigraphic units were compared using product-moment correlations. In this way, we could check for the presence of common (i.e. non-specific) external factors driving $\delta^{13}C$ changes over time. Similarly, pair-wise species combinations involving modern material were also compared by means of product-moment correlations, although in this case the basis for comparison was the common geographical origin of samples. Differences among treatments and their interactions in the ANOVA, and correlation coefficients were considered statistically significant at $P \leq 0.05$. All analyses were performed using standard SAS-STAT procedures (SAS Institute Inc., Cary, NC, USA).

Results

$\Delta^{13}C$ response to annual and seasonal precipitation in Q. ilex and P. halepensis

The linear regression models relating annual precipitation to wood $\Delta^{13}C$ are shown in Table 2. $\Delta^{13}C$ records from *P. halepensis* were better predictors of annual precipitation than those from *Q. ilex*. Splitting the total annual period into two complementary seasons (January–August and September–December) yielded species-specific differences on the explanation of precipitation from wood $\Delta^{13}C$ (Table 2). In particular, the regression models indicated a better prediction of January–August precipitation ($P_{J\text{-}A}$) from *P. halepensis* $\Delta^{13}C$, whereas September–December precipitation ($P_{S\text{-}D}$) was better inferred through *Q. ilex* $\Delta^{13}C$ (coefficients of determination, Table 2). For both species, the best seasonal models fitted the precipitation values better than their corresponding annual

Table 2. Linear regression models predicting annual, January–August and September–December precipitation from $\Delta^{13}C$ of modern samples of *Pinus halepensis* and *Quercus ilex*.

	P. halepensis			*Q. ilex*		
Precipitation	*n*	Model	R^2	*n*	Model	R^2
Annual	23	$145.6 \times \Delta^{13}C - 1862.4$	0.59	31	$116.8 \times \Delta^{13}C - 1505.4$	0.47
January–August	23	$93.0 \times \Delta^{13}C - 1216.2$	0.63	31	$60.8 \times \Delta^{13}C - 732.3$	0.33
September–December	23	$52.6 \times \Delta^{13}C - 646.2$	0.39	31	$56.0 \times \Delta^{13}C - 773.1$	0.57

n, Number of samples.

models, suggesting a more precise prediction of this climatic variable combining bi-specific $\Delta^{13}C$ data.

Interspecific comparison of $\Delta^{13}C$ in modern samples

To investigate species co-occurrence patterns of $\Delta^{13}C$, the subset of modern samples of different species (either forest trees or cereals) that were found to co-occur in particular geographical settings were subjected to correlation analysis involving all pair-wise species combinations. The relationship between $\Delta^{13}C$ of *Q. ilex* and *P. halepensis* was positive and significant ($r = 0.59$; Fig. 2a). Similarly, the $\Delta^{13}C$ records of *H. vulgare* and *T. aestivum* were positively related ($r = 0.97$; Fig. 2b). The tighter association between $\Delta^{13}C$ values of cereals agrees with the highly coincident temporal frames of grain filling for both species (April–May). When comparing $\Delta^{13}C$ records of species belonging to the two functional groups (graminoids and forest trees), the relationships were always positive and either marginally significant (for *P. halepensis* vs. *H. vulgare*, $r = 0.56$, $P < 0.1$) or significant (for all other combinations) (Fig. 3). These associations, however, could be impaired by the low number of common combinations available for comparison in most cases, ranging from $n = 4$ (for *Q. ilex* vs. *T. aestivum*) to $n = 10$ (for *P. halepensis* vs. *H. vulgare*).

Effect of experimental carbonization on Q. ilex $\delta^{13}C$

For control (untreated) samples, $\delta^{13}C$ showed considerable variation, ranging from −27.50 to −23.81‰ (mean = -25.54 ± 0.82‰; mean ± SD), whereas %C showed less variability (45.4 ± 0.5%) (Fig. 4a). The ANOVAs for the experimentally charred wood revealed a lack of significant differences between intact and powdered segments exposed to distinct temperatures for both $\delta^{13}C$ and %C. By contrast, the

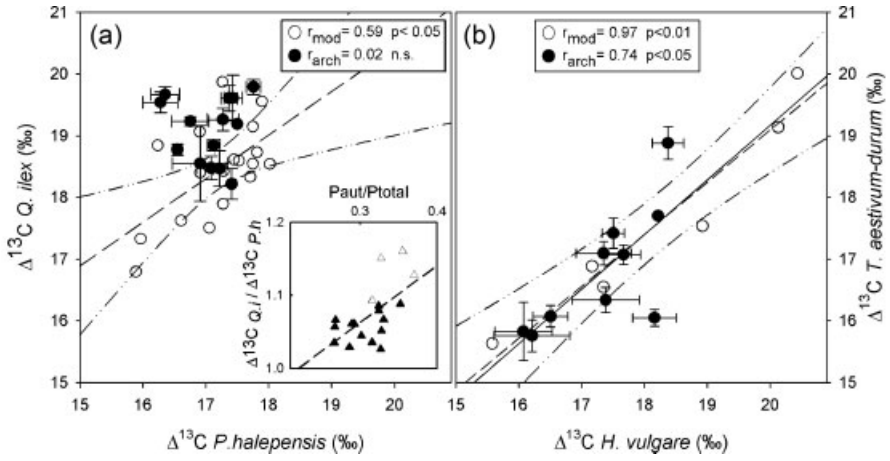

Figure 2. Relationship between (a) $\Delta^{13}C$ of *P. halepensis* and $\Delta^{13}C$ of *Q. ilex*; and (b) $\Delta^{13}C$ of *H. vulgare* and $\Delta^{13}C$ of *T. aestivum-durum*, for archaeological samples (filled symbols) and modern samples (open symbols). Error bars indicate standard error. Inset: relationship between the ratio of autumn to total precipitation and the ratio between $\Delta^{13}C$ of *Q. ilex* and $\Delta^{13}C$ of *P. halepensis* in modern samples.

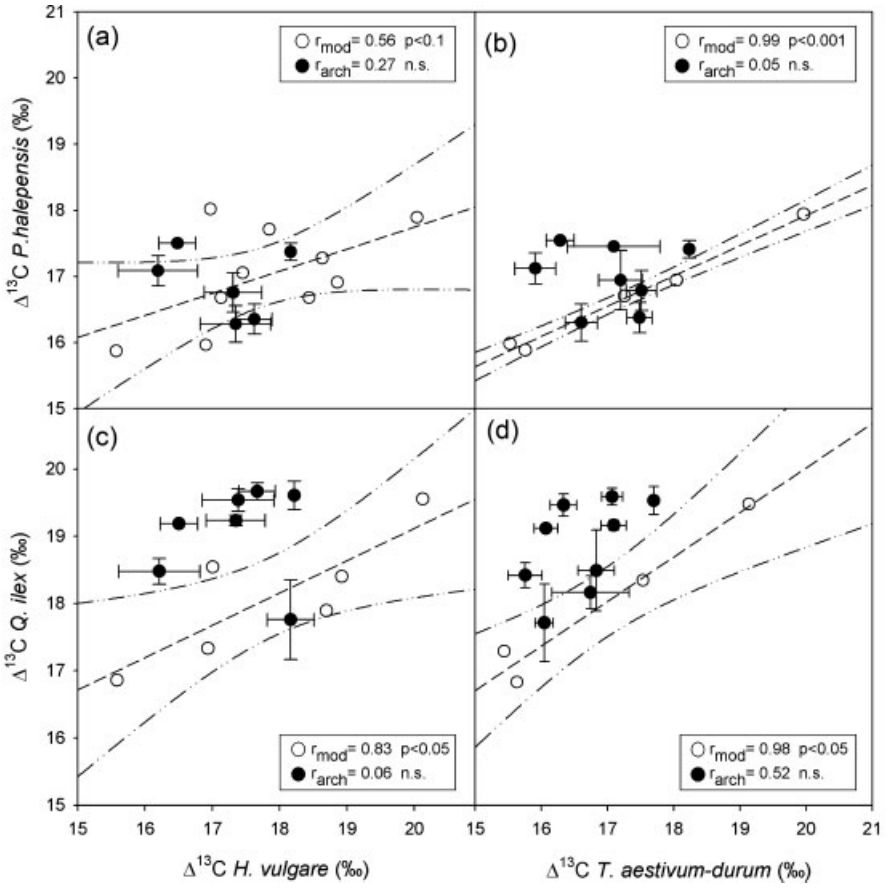

Figure 3. Relationship between (a) $\Delta^{13}C$ of *Q. ilex* and $\Delta^{13}C$ of cereal grains; and (b) $\Delta^{13}C$ of *P. halepensis* and $\Delta^{13}C$ of cereal grains, for archaeological and modern samples of *H. vulgare* (filled and open circles, respectively) and for archaeological and modern samples of *T. aestivum-durum* (filled and open triangles, respectively). Error bars indicate standard error.

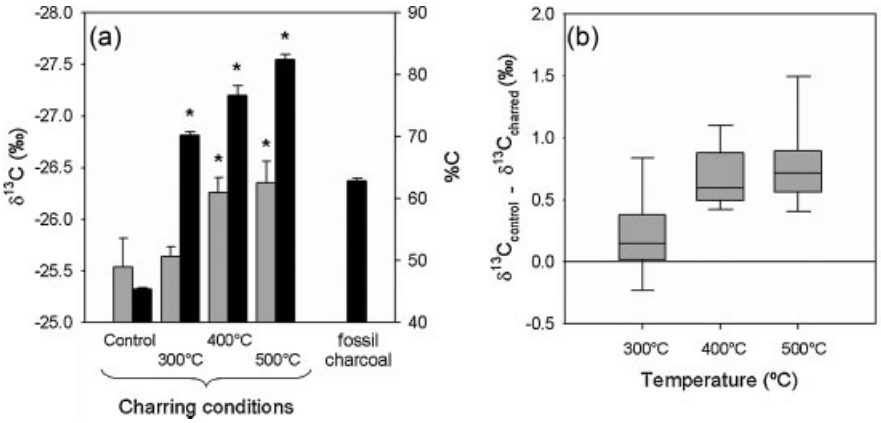

Figure 4. (a) Mean (and standard errors) for $\Delta^{13}C$ (shaded bars) and %C (black bars) in Holm oak wood under control conditions and after the carbonization treatments at 300, 400 and 500°C, and in archaeological samples (%C only). (b) Whisker plots showing the distribution of differences between $\Delta^{13}C$ of control and charred samples at 300, 400 and 500°C.

effect of charring temperature on these variables was significant, accounting for about 11 and 83% of the total variation for $\delta^{13}C$ and %C, respectively. In this regard, the geographical origin of samples was the most relevant factor explaining variation in $\delta^{13}C$, being far less important for %C (about 40 and 7% of the total variation, respectively). A progressive increase of %C with rising charring temperatures was observed, ranging from $70.3 \pm 2.0\%$ (300°C) to $82.5 \pm 2.4\%$ (500°C), together with a parallel decrease in $\delta^{13}C$ values (Fig. 4a). In particular, ANOVAs for pair-wise differences between control and treated samples revealed no significant impact of carbonization at 300°C on $\delta^{13}C$ (mean difference $= 0.19 \pm 0.25$‰), but a significant effect in samples charred at both 400°C (0.68 ± 0.18‰) and 500°C (0.84 ± 0.28‰) (Fig. 4b). In contrast, carbonization significantly increased %C of samples as compared with controls, irrespective of the charring treatment (Fig. 4a).

The mean %C of archaeological charcoal was $62.9 \pm 4.2\%$. This value was significantly higher than the carbon concentration of control samples used in the charring experiment (Student's *t*-test; $t = 31.91$, $P < 0.001$), but lower than results of the charring treatment at either 300°C ($t = 8.38$, $P < 0.001$) or higher temperatures. From these observations and the non-significant effect of carbonization at 300°C as compared with control conditions, it was concluded that the impact of carbonization on $\delta^{13}C$ had been negligible in this collection of archaeobotanical *Q. ilex* specimens.

$\Delta^{13}C$ in archaeobotanical remains

The $\Delta^{13}C$ values of archaeological samples, calculated from $\delta^{13}C_{air}$ and either raw $\delta^{13}C$ records (for *H. vulgare*, *T. aestivum/durum* and *Q. ilex/coccifera*) or estimated wood $\delta^{13}C$ after correcting for the impact of carbonization (for *P. halepensis*), varied considerably across sites, periods and species. Overall, $\Delta^{13}C$ values of *Q. ilex* ranged from 17.76 to 19.79‰, with a mean of 19.04 ± 0.44‰, whereas the mean $\Delta^{13}C$ of *P. halepensis* was 17.07 ± 0.54‰ (range 16.28–17.76‰). An interspecific comparison of charcoal $\Delta^{13}C$ records originating from common stratigraphic units revealed no clear pattern of common external factors causing variation in $\Delta^{13}C$ over the last seven millennia, in contrast to the significant linear relationship observed for modern samples when comparing tree species (Fig. 2a). Clearly, most *Q. ilex* remains had higher than expected $\Delta^{13}C$ values, taking the present-day association obtained between both species (Fig. 2a) as a basis for comparison. As $\Delta^{13}C$ of *Q. ilex* was found primarily to reflect changes in autumn precipitation (see above), this observation could indicate an increased importance of this season's contribution to the annual precipitation in the past. To check this hypothesis further, the ratio of autumn to annual precipitation was related to the ratio of *Q. ilex* to *P. halepensis* $\Delta^{13}C$ values for the set of modern samples sharing a common geographical origin (Fig. 2a). A positive association was found between the two variables ($r = 0.61$, $P < 0.01$) (Fig 2a, inset). In addition, the modern material having $\Delta^{13}C$ records similar to those of ancient charcoals (i.e. four points falling outside the upper confidence limit of the relationship between modern $\Delta^{13}C$ records; open triangles in Fig. 2a, inset) was found to have autumn to annual precipitation ratios higher than the remaining modern samples (one-tailed Student's *t*-test; $t = 2.41$, $P = 0.014$).

In clear contrast to the lack of an association between $\Delta^{13}C$ records of forest tree charcoals, contemporary $\Delta^{13}C$ values of *H. vulgare* and *T. aestivum/durum* charred grains were significantly related ($r = 0.74$, $P < 0.05$), with a similar range of variability for both cereal species (mean values, for *H. vulgare* $= 17.27 \pm 1.19$‰, for *T. aestivum/durum* $= 16.67 \pm 1.16$‰) (Fig. 2b). Likewise, the slope and intercept terms of the linear relationship did not differ statistically between modern and ancient material according to analysis of covariance testing for heterogeneity of slopes. Finally, pair-wise comparisons of $\Delta^{13}C$ records of species belonging to the two functional groups provided non-significant associations in all cases (Fig. 3). This outcome differed from the positive (and significant) relationships involving $\Delta^{13}C$ records of modern material (Fig. 3). In particular, ancient samples of *Q. ilex* exhibited a higher than expected $\Delta^{13}C$ according to the association found in modern material between this species and either graminoid species (Fig. 3c,d).

Past trends of water availability from $\Delta^{13}C$ of archaeobotanical material

Changes in $\Delta^{13}C$ over the period 5000 BC to AD 600 are shown in Fig. 5 for each functional group. High $\Delta^{13}C$ values of *Q. ilex* charcoal were observed between 600 BC and AD 200 whereas low $\Delta^{13}C$ values were found around 3000 BC. For *P. halepensis*, low $\Delta^{13}C$ values were detected principally during the second half of the first millennium BC (Fig. 5a). Overall, the correspondence between $\Delta^{13}C$ trends was good, with the exception of the period 400 BC to AD 100, in which a high $\Delta^{13}C$ for *Q. ilex* was coupled with a low $\Delta^{13}C$ for *P. halepensis* (Fig. 5a). As a consequence, the ratio of *Q. ilex* to *P. halepensis* $\Delta^{13}C$ values was higher than 1.15 for this period, indicating an enhanced contribution of autumn rainfall to the annual precipitation budget, as suggested in Fig. 2(a, inset). In turn, the cereal species presented a much better agreement in the evolution of their $\Delta^{13}C$ values over time, with low records detected in three different periods (≈5000 BC, ≈1800 BC and

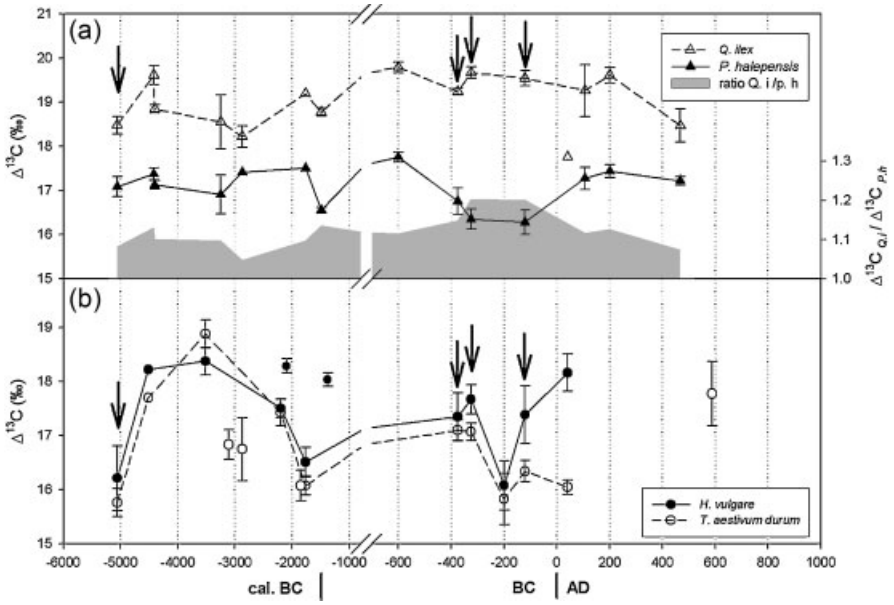

Figure 5. Evolution of $\Delta^{13}C$ for (a) charcoal samples of *P. halepensis* (filled triangles) and *Q. ilex* (open triangles) and (b) cereal remains of *H. vulgare* (filled circles) and *T. aestivum-durum* (open circles) from the Neolithic to Visigoth periods in the studied area. The arrows indicate samples of both cereals and tree species originating from the same stratigraphic unit. Plotted values not included in trend lines correspond to samples without coeval equivalents of the same functional group.

200 BC) alternating with high values achieved mainly in the 5th and 4th millennia BC and around 350 BC. The tight association between *H. vulgare* and *T. aestivum/durum* detected over time was only interrupted around the onset of the current era, a time in which barley showed a much larger $\Delta^{13}C$ (≈2‰) than wheat (Fig. 5b).

The best seasonal models from Table 2 were subsequently applied to $\Delta^{13}C$ values of archaeological charcoal to infer past trends in both seasonal and annual precipitation. The estimated $P_{J\text{-}A}$ from *P. halepensis* ranged from 298 to 435 mm (mean 372 ± 42 mm). The estimated values for archaeological samples were considerably higher than the values recorded for the present day, averaged across archaeological sites ($P_{J\text{-}A} = 290 \pm 44$ mm). In turn, the estimated $P_{S\text{-}D}$ from *Q. ilex* ranged from 221 to 335 mm (mean = 291 ± 34 mm), which again exceeded the values recorded for the present day averaged across archaeological sites ($P_{S\text{-}D} = 236 \pm 51$ mm). To avoid possible biases in the comparison with present conditions arising from differences in the geographical origin of archaeological samples, estimated seasonal values of precipitation were corrected for current climatic records at each site, thus providing differences in seasonal precipitation between the past and present (Fig. 6a). Mean differences in $P_{J\text{-}A}$ and $P_{S\text{-}D}$ were mostly positive, with means of 81 ± 29 and 55 ± 56 mm, respectively. Altogether, the summed differences in past to present seasonal precipitation always gave above-zero annual estimates, ranging from 11 to 238 mm, with a mean of 152 ± 74 mm. Ratios of past to present annual precipitation for each site–period combination are also represented in Fig. 6(a). The average ratio was 1.31 (i.e. an average increase of 31% in past precipitation), with estimates ranging from 1.02 (3249 cal a BC) to 1.50 (1764 cal a BC).

The models relating grain $\Delta^{13}C$ and WI during grain filling were also applied to $\Delta^{13}C$ values of charred grains. The estimated WI from *H. vulgare* ranged from 84 to 177 mm (mean = 135 ± 34 mm); in turn, the estimated WI from *T. aestivum/durum* ranged from 71 to 220 mm (mean = 112 ± 40 mm). Both exceeded the values recorded for present-day precipitation during grain filling averaged across sites ($WI = 70 \pm 22$ mm). WI estimates were corrected for current precipitation records at each archaeological site, hence providing differences in WI between the past and present (Fig. 6b). Mean differences in WI were also mainly positive, with a mean of 51 ± 34 mm. Ratios of past to present WI for

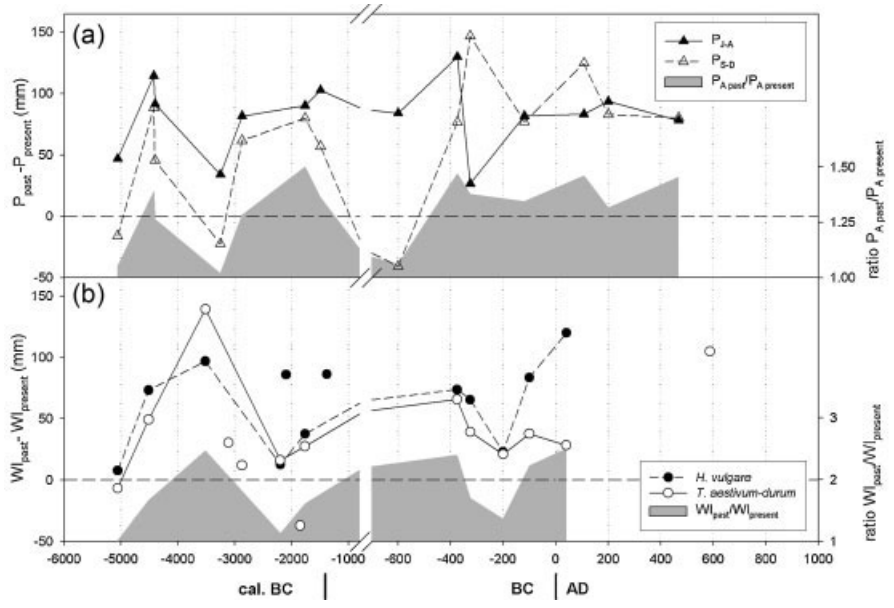

Figure 6. Evolution of differences between (a) estimated past and present precipitation, for the January–August period, inferred from $\Delta^{13}C$ values of *P. halepensis* remains (filled triangles), and for the September–December period, inferred from $\Delta^{13}C$ values of *Q. ilex* remains (open triangles) and (b) estimated past and present water inputs during grain filling of *H. vulgare* (filled circles) and *T. aestivum-durum* (open circles) from the Neolithic to Visigoth period in the studied area. Water inputs during grain filling were calculated according to Ferrio *et al.* (2005). Plotted values not included in trend lines correspond to samples without coeval equivalents of the same functional group.

each site–period combination are represented in Fig. 6(b). The average ratio was 1.80 (i.e. average increase of 80% in past WI), with estimates ranging from 1.01 (5058 a.n.e.) to 2.49 (41 n.e.).

Discussion

Interspecific differences in $\Delta^{13}C$ sensitivity to water availability

Carbon isotope ratios of *P.halepensis* were better predictors of annual precipitation than those of *Q. ilex*, in agreement with previous results for the region (Ferrio *et al.*, 2003). In general, a strong precipitation signal in the $\Delta^{13}C$ of structural carbon compounds (i.e. wood) is expected when water is limiting plant function (Warren *et al.*, 2001). Interspecific differences in the seasonal dependence of $\Delta^{13}C$ have also been reported (Walcroft *et al.*, 1997; Ferrio *et al.*, 2003; Loader *et al.*, 2003; Helle and Schleser, 2004). Indeed, our results confirm the existence of a differential sensitivity to water availability in Aleppo pine and Holm oak. The complementary bi-specific seasonal models for precipitation (January–August for *P. halepensis*, September–December for *Q. ilex*) provided a better prediction of total precipitation than each mono-specific annual model (Table 2).

In concordance with the dependence on rainfall of Mediterranean conifers (Valentini *et al.*, 1992), *P. halepensis* has shown significant associations with monthly precipitation throughout the year (Ferrio *et al.*, 2003). It is highly responsive to short-term meteorological fluctuations (Hemming *et al.*, 2001), and this signal is well preserved in tree rings, as demonstrated by the close link between average leaf-level CO_2 exchange and carbon deposition in the stem over seasonal scales (Klein *et al.*, 2005). *P. halepensis* shows two periods with reduced cambial activity: one is defined by the summer drought and the other by low winter temperatures (Liphschitz and Lev-Yadun, 1986). This translates on average into growth rate maxima occurring from March to June in the Iberian Peninsula (Pardos *et al.*, 2003). Together, these morphophysiological features can explain the superior predictive ability of $\Delta^{13}C$ for inter-site precipitation from January to August as compared with annual values.

Conversely, *Q. ilex* is a deep-rooted species that depends on rainfall supplies but also on very effective water uptake (Valentini *et al.*, 1992). This performance is supported by the strong seasonal precipitation signal stored in wood $\Delta^{13}C$, corresponding to the two annual peaks of precipitation of the western Mediterranean (autumn and late winter to spring) (Aguilera *et al.*, 2009). A recent study involving two Mediterranean evergreen oaks (*Q. ilex* and *Q. suber*) has demonstrated the importance of autumn rewatering to explain the fast recovery in photosynthesis following the summer drought (Vaz *et al.*, 2010). The better fit of the seasonal model explaining September–December precipitation as compared with the annual model supports the high sensitivity to autumn precipitation for this species. When $\Delta^{13}C$ records of *Q. ilex* and *P. halepensis* in modern samples were compared, the association was significant but weak, highlighting the differential water-use strategy embraced by each species. With regard to these results, the ratio of *Q. ilex* to *P. halepensis* $\Delta^{13}C$ values appears to be a useful indicator of rainfall seasonality in modern samples, and may be used to aid interpreting changes in intra-annual dynamics of past precipitation over time.

Regarding cereals, a tight association arises when rain-fed wheat and barley are compared for grain $\Delta^{13}C$ in modern samples, corroborating the similar dependence of their carbon isotope signatures from WI during grain filling (i.e. early spring, April–May). This dependence has been used to discriminate between climate-derived and anthropogenic effects (water management practices) on ancient crops, assuming that discrepancies from the general trend between species would be indicative of differential crop management (Ferrio *et al.*, 2005; Aguilera *et al.*, 2008; Heaton *et al.*, 2009). In the present study, however, the close relationship between archaeological wheat and barley samples, in agreement with modern data on co-occurring crops, does not provide evidence of selective crop management.

Impact of charring on Q. ilex $\delta^{13}C$

The lack of significant shifts in the original wood $\delta^{13}C$ for the lowest temperature (300°C), along with the observation that charred wood becomes depleted in ^{13}C but progressively enriched in carbon under higher temperatures, agrees with a number of studies (Czimczik *et al.*, 2002; Harden *et al.*, 2004; Turney *et al.*, 2006). Organic %C of wood increases with increasing temperature due to the variable thermal tolerances of different wood compounds and the fastest loss of other elements, such as O or H (Kollmann, 1955). Consequently, the selective losses of carbon compounds (i.e. resins, lignin, celluloses and others), with dissimilar $\delta^{13}C$ (Turekian *et al.*, 1998; Ferrio and Voltas, 2005), is the most likely explanation for the observed experimental shifts in $\delta^{13}C$. Previous studies on *P. halepensis* showed a progressive decrease in $\delta^{13}C$ with increasing charring temperature, negatively correlated to the increase in %C, which allowed development of a correction equation based on %C changes (Ferrio *et al.*, 2006). In contrast, for *Q. ilex* we have found an uncoupling between the strong initial changes in %C and the weak effect on $\delta^{13}C$, the latter showing significant effects only at temperatures above 400°C. Remarkably, the average %C of archaeological samples (lower than the value attained in experimental charring at 300°C) indicates a lower degree of carbonization than required for altering the original $\delta^{13}C$ in *Q. ilex*. This is consistent with the relatively low temperatures (<450°C) typically reached in natural fires (Whelan, 1995). Overall, our results indicate that $\delta^{13}C$ of *Q. ilex* charcoal remained largely unaffected, hence preserving its original climatic signal.

Precipitation seasonality and $\Delta^{13}C$ in archaeobotanical remains

The good correspondence between $\Delta^{13}C$ trends of *P. halepensis* and *Q. ilex* for the period 5000 BC to 1500 BC (Fig. 5) points to the absence of relevant changes in precipitation seasonality over the mid-Holocene (roughly 7000 to 4000 years ago) in the western Mediterranean. Also, the ratio of *Q. ilex* to *P. halepensis* $\Delta^{13}C$ values, varying between 1.05 and 1.1, suggests a similar contribution of autumn rainfall to the annual precipitation as found at present (cf. Fig. 2a, inset). In contrast, the contribution of autumn rainfall to the total water budget appears enhanced for the second half of the first millennium BC (400 BC to AD 100), in which a high $\Delta^{13}C$ for *Q. ilex* was coupled with a low $\Delta^{13}C$ for *P. halepensis* (ratio of *Q. ilex* to *P. halepensis* $\Delta^{13}C$ exceeding 1.15).

The parallel trends over time in $\Delta^{13}C$ of charred grains suggest the alternating existence of drier (≈5000 BC, ≈1800 BC and 200 BC) and wetter springs (≈3500 BC, ≈350 BC). These contrasting phases are supported by other palaeoenvironmental proxies. The low pollen ratio of deciduous broadleaved to evergreen sclerophyllous trees at Salinas, south-eastern Spain (Jalut *et al.*, 2000), points to an arid phase around 5000 BC, whereas high lake level records in south-western Spain suggest a humidity optimum between 4000 and 3800 BC (Magny *et al.*, 2002). Jalut *et al.* (2000) also reports on phases of minimum

pollen ratios at about 1800 BC and for the period 900 BC to AD 220, which are both coincident with the low $\Delta^{13}C$ detected for cereals. The relative scarcity of strictly contemporary records of cereals and forest trees (i.e. from the same stratigraphic unit, arrows in Fig. 5a,b) makes a direct comparison of $\Delta^{13}C$ trends difficult. For those cases in which such assessment was possible, there was not a clear consistency in changes of $\Delta^{13}C$ records. For instance, low values were consistently found at 5058 BC, and high values at 375 BC and 325 BC (but only for cereals and *Q. ilex*). Conversely, high values for *Q. ilex* and *H. vulgare* were detected along with low values for *P. halepensis* and *T. aestivum* at AD 120. These results probably reveal further complexities in the interpretation of seasonal precipitation patterns owing to the limited availability of archaeobotanical remains covering the mid- and late Holocene. This is particularly evident for cereal grains, which only track spring climatic conditions during a single year.

Changes in precipitation from the Early Neolithic to the Roman period

We estimated differences between past and present-day precipitation from 5000 BC to AD 450 by comparing modelled precipitation in the past (derived from charcoal $\delta^{13}C$) with the current average rainfall for each archaeological site. Compared with present conditions, estimated spring–summer precipitation ($P_{J\text{-}A}$) was consistently higher in the past, whereas autumn–winter precipitation ($P_{S\text{-}D}$) showed alternatively higher and lower values. Nevertheless, estimated annual precipitation was consistently higher than at present throughout the studied period, in agreement with previous studies on the western Mediterranean (Terral and Mengual, 1999; Carrión *et al.*, 2001; Ferrio *et al.*, 2007).

Comparing the two seasonal periods predicted by our models, past minus present precipitation was probably higher from January to August than from September to December in the period 5000 BC to 400 BC, but a seasonal precipitation change occurred afterwards, leading to similar values for both seasonal precipitation differences from 400 BC to AD 450. These findings agree with a macrophysical climate model (Bryson and DeWall, 2007) that estimated monthly precipitation and rain-event intensity for the last 12 000 years for the city of Alcoi (Miller *et al.*, 2009; McClure *et al.*, 2009), in the same area as the studied sites. This model estimated a progressive decrease (but strong instability) in July precipitation from ca. 3000 BC to ca. 500 BC, whereas both January precipitation and the intensity of rain-events during September would have increased during this period. Thus, our estimated seasonal changes could be explained by the increase in intense rainfall episodes along the Mediterranean coast during the Holocene, which can be attributed to an enhancement of the African monsoon (Stevens *et al.*, 2001).

Although precipitation was generally higher than present throughout the studied period, two main dry episodes were observed, around 4000–3000 BC and 1000–500 BC. The first period coincides with one of the Holocene's cooling phases, which resulted in high lake levels in Central Europe (Magny, 1999), but caused an aridification phase in the Mediterranean, as described by Jalut *et al.* (2000). Our results partly agree with those derived from the aforementioned macrophysical model, which predicted low rainfall in January and September, but relatively high precipitation in July, which afterwards decreased from ca. 3000 BC to 2000 BC (Miller *et al.*, 2009). As our prediction model from *P. halepensis* combine winter, spring and most summer months, the decrease in January precipitation may have exceeded a possible increase in summer rainfall, leading to an overall reduction in $P_{J\text{-}A}$.

The second dry episode (ca. 1000–500 BC) showed an important decrease in $P_{S\text{-}D}$ as compared with present conditions, but not in $P_{J\text{-}A}$, suggesting a sharp decrease in autumn precipitation, but little change in spring–summer rainfall. These results agree with low precipitation values reported for this period in the Central Ebro Basin (Ferrio *et al.*, 2006), as well as with the low $\Delta^{13}C$ values in oaks from the western Mediterranean (Vernet *et al.*, 1996; Ferrio *et al.*, 2005). This period coincides with the Cold Iron Age Epoch, which could have been drought-prone in the Iberian Peninsula, contrasting with the increased rainfall recorded in Central Europe (Magny, 1999; Jalut *et al.*, 2000; Ferrio *et al.*, 2007; Aguilera *et al.*, 2009; McClure *et al.*, 2009).

Regarding cereal $\Delta^{13}C$, maximum difference between past and present WI during grain filling coincided for wheat and barley ca. 3500 BC, in agreement with an increase in spring rains detected by lake-level records during the mid-Holocene (6500–4500 cal a BP) (Stevens *et al.*, 2001). Observing similar differences in WI throughout the mid- and late Holocene for both cereals, strong anthropogenic or agronomic effects on grain $\Delta^{13}C$ can be ruled out. Thus, the $\Delta^{13}C$ data from trees and crops can be used together to further investigate changes in climate seasonality through time. An important proportion of the differences in $P_{J\text{-}A}$ between past and present conditions may stem from changes in mid-spring precipitation, which is the main period determining the $\Delta^{13}C$ of cereal grains, and thus WI estimates (Araus *et al.*, 1997; Ferrio *et al.*, 2005). However, $P_{J\text{-}A}$ and WI provided (apparently) contradictory results for 3500 BC, when the maximum difference in WI between past and present was detected. This is in agreement with carbonate $\delta^{18}O$ values from Lake Medina in the south-western part of the Iberian Peninsula, in which high spring precipitation may be reflected in high $\delta^{18}O$ values (Roberts *et al.*, 2008). These changes in precipitation seasonality between winter and spring might hinder the interpretation of isotope records and thus they make a case for the development of multi-species isotope values and complementary proxies to infer climatic changes.

Conclusions

The multispecific assessment of $\Delta^{13}C$ changes in the archaeobotanical record has provided additional insight into the characterization of Holocene climate. In particular, this study has shown how a combination of species holding different (and complementary) environmental signals can contribute to a wider knowledge of seasonal precipitation dynamics at the local level. The abundance of charcoal remains in the eastern Iberian Peninsula from species that exhibit contrasting strategies to cope with drought, along with the analysis of charred grains, has facilitated this task. In particular, past spring–summer precipitation was always higher than at present, whereas autumn and early winter precipitation showed stronger fluctuations, being alternatively much higher or lower in the past than today. The large contribution of autumn precipitation to the annual water budget was noteworthy during the second half of the first millennium BC and at the beginning of the current era, suggesting an increase in torrential rainfall events comparable with those mainly occurring at the present day during autumn in this region. Also, the incidence of dry episodes (fourth millennium BC and first half of the first millennium BC) was associated with the scarcity of autumn precipitation. Alternative species can contribute to widen the palaeoenvironmental record in the future, although this will be subject to the abundance of archaeobotanical remains in the area of interest and the proper ecophysiological understanding of the recorded isotopic signal.

Supporting information

Additional supporting information can be found in the online version of this article:

Table S1. Main geographic and environmental characteristics of archaeological sites, chronology and AMS data references.

Please note: This supporting information is supplied by the authors, and may be re-organized for online delivery, but is not copy-edited or typeset by Wiley-Blackwell. Technical support issues arising from supporting information (other than missing files) should be addressed to the authors.

Acknowledgements. This work was partially supported by the DGI project CGL2009-13079-C02-01 and the ERC-Advanced grant 230561 (AGRIWESTMED). We acknowledge Ernestina Badal, Elena Grau and Yolanda Carrión for charcoal identification and P. Sopeña for technical assistance. M.A. has a PhD fellowship from the Spanish Ministry of Science and Innovation and J.P.F. is supported by a postdoctoral contract from the ''Ramon y Cajal'' programme (MCINN).

Abbreviation. WI, water input.

References

Aguilera M, Araus JL, Voltas J, *et al*. 2008. Stable carbon and nitrogen isotopes and quality traits of fossil cereal grains provide clues on sustainability at the beginnings of Mediterranean agriculture. *Rapid Communications in Mass Spectrometry* **22**: 1653–1663.

Aguilera M, Espinar C, Ferrio JP, *et al*. 2009. A map of autumn precipitation for the third millennium BP in the Eastern Iberian Peninsula from charcoal carbon isotopes. *Journal of Geochemical Exploration* **102**: 157–165.

Araus JL, Buxó R. 1993. Changes in carbon isotope discrimination in grain cereals from the north-western Mediterranean basin during the past seven millenia. *Australian Journal of Plant Physiology* **20**: 117–128.

Araus JL, Febrero A, Buxó R, *et al*. 1997. Changes in carbon isotope discrimination in grain cereals from different regions of the western Mediterranean basin during the past seven millennia. Palaeoenvironmental evidence of a differential change in aridity during the late Holocene. *Global Change Biology* **3**: 107–118.

Araus JL, Febrero A, Catala M, *et al*. 1999. Crop water availability in early agriculture: evidence from carbon isotope discrimination of seeds from a tenth millennium BP site on the Euphrates. *Global Change Biology* **5**: 201–212.

Araus JL, Villegas D, Aparicio N, *et al*. 2003. Environmental factors determining carbon isotope discrimination and yield in durum wheat under Mediterranean conditions. *Crop Science* **43**: 170–180.

Barriendos M, Llasat MC. 2003. The case of the 'Malda' Anomaly in the Western Mediterranean basin (AD 1760–1800): an example of a strong climatic variability. *Climatic Change* **61**: 191–216.

Bryson RA, DeWall KM. 2007. An introduction to the archaeoclimatology macrophysical climate model. In *A Paleoclimatology Workbook: High Resolution, Site-Specific, Macrophysical Climate Modeling*, Bryson RA, DeWall KM (eds). The Mammoth Site: Hot Springs, SD; 3–11.

Buxó R, Piqué R. 2008. *Arqueobotánica. Los usos de las plantas en la península Ibérica*. Ariel Prehistoria: L'Hospitalet de Llobregat (Barcelona).

Carrión JS, Munuera M, Dupré M, Andrade A. 2001. Abrupt vegetation changes in the Segura Mountains of southern Spain throughout the Holocene. *Journal of Ecology* **89**: 783–797.

Carrión JS, Van Geel B. 1999. Fine- resolution Upper Weichselian and Holocene palynological record from Navarrés (Valencia, Spain) and a discussion about factors of Mediterranean forest succession. *Review of Palaeobotany and Palynology* **106**: 209–236.

Cortijo ML. 2007. Los árboles silvestres en la Iberia de Estrabon. *Zephyrus* **60**: 209–219.

Czimczik CI, Preston CM, Schmidt MWI, *et al*. 2002. Effects of charring on mass, organic carbon, and stable carbon isotope composition of wood. *Organic Geochemistry* **33**: 1207–1223.

DeNiro MJ, Hastorf CA. 1985. Alteration of $^{15}N/^{14}N$ and $^{13}C/^{12}C$ ratios of plant matter during the initial stages of diagenesis: studies utilizing archaeological specimens from Peru. *Geochimica et Cosmochimica Acta* **49**: 97–115.

Dunkeloh A, Jacobeit J. 2003. Circulation dynamics of Mediterranean precipitation variability 1948–98. *International Journal of Climatology* **23**: 1843–1866.

Dupouey JL, Leavitt SW, Choisnel E, Jourdain S. 1993. Modelling carbon isotope fractionation in tree rings based on effective evapotranspiration and soil water status. *Plant Cell Environmental* **16**: 939–947.

Farquhar GD, O'Leary MH, Berry JA. 1982. On the relationship between carbon isotope discrimination and the inter-cellular carbon-dioxide concentration in leaves. *Australian Journal of Plant Physiology* **9**: 121–137.

Fernández S, Fuentes N, Carrión JS, *et al*. 2007. The Holocene and Upper Pleistocene pollen sequence of Carihuela Cave, southern Spain. *Geobios* **40**: 75–90.

Ferrio JP, Alonso N, López JB, *et al*. 2006. Carbon isotope composition of fossil charcoal reveals aridity changes in the NW Mediterranean Basin. *Global Change Biology* **12**: 1253–1266.

Ferrio JP, Araus JL, Buxó R, *et al*. 2005. Water management practices and climate in ancient agriculture: inference from the stable isotope composition of archaeobotanical remains. *Vegetation History and Archaeobotany* **14**: 510–517.

Ferrio JP, Bertran E, Nachit MM, *et al*. 2001. Near infrared reflectance spectroscopy as a potential surrogate method for the analysis of $\Delta^{13}C$ in mature kernels of durum wheat. *Australian Journal or Agricultural Research* **52**: 809–816.

Ferrio JP, Florit A, Vega A, *et al*. 2003. $\Delta^{13}C$ and tree ring width reflect different drought responses in *Quercus ilex* and *Pinus halepensis*. *Oecologia* **137**: 512–518.

Ferrio JP, Voltas J. 2005. Carbon and oxygen isotope ratios in wood constituents of *Pinus halepensis* as indicators of precipitation, temperature and vapour pressure deficit. *Tellus Series B-Chemical and Physical Meteorology* **57B**: 164–173.

Ferrio JP, Voltas J, Alonso N, Araus JL. 2007. Reconstruction of climate and crop conditions in the past based on the carbon isotope signature of archaeobotanical remains. In *Isotopes as Indicators of Ecological Change*, Dawson TE, Siegwolf R (eds). Elsevier Academic Press: New York; 319–332.

Flanagan LB, Ehleringer JR, Marshall JD. 1992. Differential uptake of summer precipitation among co-occurring trees and shrubs in a pinyon-juniper woodland. *Plant Cell Environmental* **15**: 831–836.

Grivet D, Sebastiani F, Alía R, Bataillon T, Torre S, Zabal-Aguirre M, Vendramin GG, González-Martínez SC. 2011. Molecular footprints of local adaptation in two Mediterranean conifers. *Molecular Biology and Evolution* **28**: 101–116.

Harden JW, Neff JC, Sandberg DV, *et al*. 2004. Chemistry of burning the forest floor during the FROSTFIRE experimental burn, interior Alaska, 1999. *Global Biogeochemistry Cycles* **18**: DOI: 10.1029/2003GB002194.

Heaton THE, Jones G, Halstead P, Tsipropoulos T. 2009. Variations in the C-13/C-12 ratios of modern wheat grain and implications for interpreting data from Bronze Age Assiros Toumba, Greece. *Journal of Archaeological Science* **36**: 2224–2233.

Helle G, Schleser GH. 2004. Beyond CO_2-fixation by Rubisco – an interpretation of $^{13}C/^{12}C$ variations in tree rings from novel intra-seasonal studies on broad-leaf trees. *Plant, Cell and Environmental* **27**: 367–380.

Hemming DL, Fritts H, Leavitt SW, *et al*. 2001. Modelling tree-ring $\delta^{13}C$. *Dendrochronologia* **19**: 23–38.

Jalut G, Esteban-Amat A, Bonnet L, *et al*. 2000. Holocene climatic changes in the Western Mediterranean, from south-east France to south-east Spain. *Palaeogeography, Palaeoclimatology, Palaeoecology* **160**: 255–290.

Jalut G, Esteban-Amat A, Mora SRI, *et al*. 1997. Holocene climatic changes in the western Mediterranean: installation of the Mediterranean climate. *Comptes Rendus de l'Académie des Sciences Série II Fascicule A-Sciences de la Terre et des Planetes* **325**: 327–334.

Jones TP, Chaloner WG. 1991. Fossil charcoal, its recognition and palaeoatmospheric significance. *Palaeogeography, Palaeoclimatology, Palaeoecology* **97**: 39–50.

Klein T, Hemming D, Lin T, *et al*. 2005. Association between tree-ring and needle $\delta^{13}C$ and leaf gas exchange in *Pinus halepensis* under semi-arid conditions. *Oecologia* **144**: 45–54.

Kollmann F. 1955. *Technologie des holzes und der holzwerkstoffe*. Springer Verlag: Heidelberg.

Korol RL, Kirschbaum MUF, Farquhar GD, Jeffreys M. 1999. Effects of water status and soil fertility on the C-isotope signature in *Pinus radiata*. *Tree Physiology* **19**: 551–562.

Liphschitz N, Lev-Yadun S. 1986. Cambial activity of evergreen and seasonal dimorphics around the Mediterranean. *IAWA Bulletin* **7**: 145–153.

Loader NJ, Robertson I, McCarroll D. 2003. Comparison of stable carbon isotope ratios in the whole wood, cellulose and lignin of oak tree rings. *Palaeogeography, Palaeoclimatology, Palaeoecology* **196**: 395–407.

Lumaret R, Mir C, Michaud H, Raynal V. 2002. Phylogeographical variation of chloroplast DNA in holm oak (*Quercus ilex* L.). *Molecular Ecology* **11**: 2327–2336.

Magny M. 1999. Lake-level fluctuations in the Jura and French subalpine ranges associated with ice-rafting events in the North Atlantic and variations in the polar atmospheric circulation. *Quaternaire* **10**: 61–64.

Magny M, Begeot C, Guiot J, Peyron O. 2003. Contrasting patterns of hydrological changes in Europe in response to Holocene climate cooling phases. *Quaternary Science Reviews* **22**: 1589–1596.

Magny M, Miramont C, Sivan O. 2002. Assessment of the impact of climate and anthropogenic factors on Holocene Mediterranean vegetation in Europe on the basis of palaeohydrological records. *Palaeogeography, Palaeoclimatology, Palaeoecology* **186**: 47–59.

Marino BD, DeNiro MJ. 1987. Isotope analysis of archaeobotanicals to reconstruct past climate: effects of activities associated with food preparation on carbon, hydrogen and oxygen isotope ratios of plant cellulose. *Journal of Archaeological Science* **14**: 537–548.

McCarroll D, Loader NJ. 2004. Stable isotopes in tree rings. *Quaternary Science Reviews* **23**: 771–801.

McClure SB, Barton CM, Jochim MA. 2009. Human behavioral ecology and climate change during the transition to agriculture in Valencia, eastern Spain. *Journal of Anthropological Research* **65**: 207–220.

Miller AMB, Oreto G, Bernabe J. 2009. Surviving the Holocene crisis: human ecological responses to the onset of the current interglacial. *Journal of Anthropological Research* **65**: 253–269.

Moreno A, Cacho I, Canals M, *et al*. 2005. Links between marine and atmospheric processes oscillating on a millennial time-scale, a multi-proxy study of the last 50000 yr from the Alboran Sea (western Mediterranean Sea), Quaternary land-ocean correlation. *Quaternary Science Reviews* **24**: 1623–1636.

Ninyerola M, Pons X, Roure JM. 2005. *Atlas Climático Digital de la Península Ibérica*. Metodología y aplicaciones en bioclimatología y geobotánica. Universidad Autónoma de Barcelona, Barcelona.

Pardos M, Climent J, Gil L, Pardos JA. 2003. Shoot growth components and flowering phenology in grafted *Pinus halepensis* Mill. *Trees-Structure and Function* **17**: 442–450.

Pérez-Obiol R, Julià R. 1994. Climatic-change on the Iberian Peninsula recorded in a 30.000-yr pollen record from Lake Banyoles. *Quaternary Research* **41**: 91–98.

Resco V, Ferrio JP, Carreira JA, *et al*. 2011. The stable isotope ecology of plant succession. *Plant Ecology and Diversity* (in press). [doi: 10.1080/17550874.2011.576708]

Roberts N, Jones MD, Benkaddour A, *et al*. 2008. Stable isotope records of Late Quaternary climate and hydrology from Mediterranean lakes: the ISOMED synthesis. *Quaternary Science Reviews* **27**: 2426–2441.

Rodó X, Baert E, Comin FA. 1997. Variations in seasonal rainfall in southern Europe during the present century: relationships with the North Atlantic Oscillation and the El Niño Southern Oscillation. *Climate Dynamics* **13**: 275–284.

Rossi S, Anfodillo T, Menardi R. 2006. Trephor: a new tool for sampling microcores from tree stems. *IAWA Journal* **27**: 89–97.

Sanchez-Goni MF, Cacho I, Turon JL, *et al*. 2002. Synchroneity between marine and terrestrial responses to millennial scale climatic variability during the last glacial period in the Mediterranean region. *Climate Dynamics* **19**: 95–105.

Stevens LR, Wright HE Jr, Ito E. 2001. Proposed changes in seasonality of climate during the Lateglacial and Holocene at Lake Zeribar, Iran. *Holocene* **11**: 747–755.

Terral JF, Mengual X. 1999. Reconstruction of Holocene climate in southern France and eastern Spain using quantitative anatomy of olive wood and archaeological charcoal. *Palaeogeography, Palaeoclimatology, Palaeoecology* **153**: 71–92.

Turekian VC, Macko S, Ballentine D, *et al*. 1998. Causes of bulk carbon and nitrogen isotopic fractionations in the products of vegetation burns: laboratory studies. *Chemical Geology* **152**: 181–192.

Turney CSM, Wheeler D, Chivas AR. 2006. Carbon isotope fractionation in wood during carbonization. *Geochimica et Cosmochimica Acta* **70**: 960–964.

Valentini R, Anfodillo T, Ehleringer JR. 1994. Water sources and carbon isotope composition ($\delta^{13}C$) of selected tree species of the Italian Alps. *Canadian Journal of Forest Research* **24**: 1575–1578.

Valentini R, Mugnozza GES, Ehleringer JR, Scarascia-Mugnozza GE. 1992. Hydrogen and carbon isotope ratios of selected species of Mediterranean macchia ecosystem. *Functional Ecology* **6**: 627–631.

Valero-Garcés BL, González-Sampériz P, Navas A, *et al*. 2004. Paleohydrological fluctuations and steppe vegetation during the last glacial maximum in the central Ebro valley (NE Spain). *Quaternary International* **122**: 43–55.

Vaz M, Pereira JS, Gazarini LC, *et al*. 2010. Drought-induced photosynthetic inhibition and autumn recovery in two Mediterranean oak species. *Tree Physiology* **30**: 946–956.

Vegas J, Perez-Gonzalez A, Ruiz Zapata B, *et al*. 2001. Environmental events occurred during the Holocene in Laguna Grande and Laguna del Hornillo lacustrine records, northwestern of the Iberian Range (Spain). *Terra Nostra* **2**: 57–60.

Vernet JL, Pachiaudi C, Bazile F, *et al*. 1996. Le $\delta^{13}C$ de charbons de bois préhistoriques et historiques méditerranéens, de 35000 BP a l'actuel. Premiers résultats. *Comptes Rendus de l'Académie des Sciences, série II a* **323**: 319–324.

Voltas J, Ferrio JP, Alonso N, Araus JL. 2008. Stable carbon isotopes in archaeobotanical remains and palaeoclimate. *Contributions to Science* **4**: 21–31.

Voltas J, Romagosa I, Lafarga A, *et al*. 1999. Genotype by environment interaction for grain yield and carbon isotope discrimination of barley in Mediterranean Spain. *Australian Journal or Agricultural Research* **50**: 1263–1271.

Walcroft AS, Silvester WB, Whitehead D, Kelliher FM. 1997. Seasonal changes in stable carbon isotope ratios within annual rings of *Pinus radiata* reflect environmental regulation of growth processes. *Australian Journal of Plant Physiology* **24**: 57–68.

Warren CR, McGrath JF, Adams MA. 2001. Water availability and carbon isotope discrimination in conifers. *Oecologia* **127**: 476–486.

Weninger B, Jöris O, Danzeglocke U. 2007. CalPal-2007: Cologne Radiocarbon Calibratrion and Palaeoclimate Research Package. http://www.calpal.de/.

Whelan RJ. 1995. *The Ecology of Fire*. Cambridge University Press: Cambridge.

Williams DG, Ehleringer JR. 2000. Intra- and interspecific variation for summer precipitation in pinyon-juniper woodlands. *Ecological Monographs* **70**: 517–537.